Climate change may alter mercury fluxes in northern hardwood forests

Yang Yang · Linghui Meng · Ruth D. Yanai · Mario Montesdeoca ·
Pamela H. Templer · Heidi Asbjornsen · Lindsey E. Rustad · Charles T. Driscoll

Abstract Soils are the largest terrestrial pool of mercury (Hg), a neurotoxic pollutant. Pathways of Hg accumulation and loss in forest soils include throughfall, litterfall, soil gas fluxes, and leaching in soil solution, all of which will likely be altered under changing climate. We took advantage of three ongoing climate-change manipulation experiments at the Hubbard Brook Experimental Forest, New Hampshire, USA: a combined growing-season warming and winter freeze-thaw cycle experiment, a throughfall exclusion to mimic drought, and a simulated ice storm experiment to examine the response of the forest Hg cycle to climatic disturbances. Across these three experiments, we compared Hg inputs in throughfall and leaf litterfall and Hg outputs in soil gas fluxes. Soil solution was measured only in the simulated ice storm experiment. We found that northern forest soils retained consistently less Hg by 16–60% in the three climate manipulations compared to the undisturbed controls ($\sim$ 7.4 µg Hg m^{-2} year^{-1}), although soils across all three experiments still served as a net sink for Hg. Growing-season soil warming and combined soil warming and winter freeze-thaw cycles had little effect on litterfall and throughfall flux, but they increased soil Hg^0 evasion by 31 and 35%, respectively, relative to the control plots. The drought plots

Responsible Editor: Edith Bai.

Y. Yang
Sierra Nevada Research Institute, University of California, Merced, Merced, CA 95340, USA

L. Meng (✉) · M. Montesdeoca · C. T. Driscoll
Department of Civil and Environmental Engineering, Syracuse University, Syracuse, NY 13244, USA
e-mail: limeng@syr.edu

R. D. Yanai
Department of Forest and Natural Resources Management, State University of New York College of Environmental Science and Forestry, Syracuse, NY 13210, USA

P. H. Templer
Department of Biology, Boston University, Boston, MA 02215, USA

H. Asbjornsen
Department of Natural Resources and the Environment, University of New Hampshire, Durham, NH 03824, USA

L. E. Rustad
Northern Research Station, USDA Forest Service, Durham, NH 03824, USA

had 5% lower litterfall Hg flux, 50% lower throughfall Hg flux, and 21% lower soil Hg^0 evasion than the control plots. The simulated ice storm had 23% higher litterfall Hg flux, 1% higher throughfall Hg flux, 37% higher soil Hg^0 evasion, and 151% higher soil Hg leaching than the control plots. These observations suggest that climate changes such as warmer soils in the growing season or more intense ice storms in winter are likely to exacerbate Hg pollution by releasing Hg sequestered in forest soils via evasion and leaching.

Introduction

Mercury (Hg) is a neurotoxic pollutant. Mercury emitted by anthropogenic and natural sources can be transported in the atmosphere (Selin et al. 2007) and deposited to remote areas. In temperate forests in North America, litterfall and throughfall (Hg washed from foliar surface during rain events) have been shown to dominate the input of Hg to forest soils (Grigal et al. 2000; St. Louis et al. 2001; Demers et al. 2007; Sheehan et al. 2006; Bushey et al. 2008). Forest soils sequester Hg because organic matter has a high affinity for Hg (Schwesig et al. 1999), but mineralization releases ionic Hg (Hg^{2+}) that can be reduced and re-emitted as elemental Hg (Hg^0) from the soil surface back to the atmosphere (Graydon et al. 2009; Denkenberger et al. 2012). The Hg^0 evaded from the soil surface or transported from other sources to the atmosphere can be taken up by leaves through their stomata (Ericksen et al. 2003; Millhollen et al. 2006; Rutter et al. 2011; Laacouri et al. 2013), where it is oxidized to Hg^{2+} and bound to thiols (Manceau et al. 2018). Forest soils can also release Hg^{2+} to receiving waters via drainage waters (Driscoll et al. 2007). The dissolved Hg leached from soils to nearby streams and lakes can be methylated and bioaccumulate up food chains, resulting in exposure to wildlife or humans (Chan et al. 2003; Chen et al. 2008). Thus, understanding the major fluxes that contribute to the

retention and loss of Hg in forest soils is important for studying Hg cycling in terrestrial ecosystems.

Meteorological variables such as temperature, precipitation, and solar radiation have been shown to influence Hg fluxes in forests. Years with less precipitation and higher air temperatures had lower Hg concentrations in litterfall in both hardwood and conifer stands at the Huntington Forest (Blackwell et al. 2014), presumably due to stomatal closure with decreased vapor pressure deficits. Months with greater precipitation had higher total Hg fluxes in throughfall (Choi et al. 2008) and soil runoff (Wang 2012) at the Huntington Forest. Litterfall and throughfall Hg fluxes are projected to increase with greater precipitation and increases in air temperatures (Smith-Downey et al. 2010). Higher soil Hg^0 evasion was observed in manipulated warmer and wetter permafrost soils in the Qinghai–Tibet Plateau in China (Ci et al. 2016b) and in manipulated warmer peatland soils in Michigan and Minnesota, USA (Haynes et al. 2017). Higher soil Hg^0 evasion was observed due to opening of the canopy after forest harvesting (Carpi et al. 2014; Mazur et al. 2014) and wildfire (Carpi et al. 2014; Melendez-Perez et al. 2014). Higher concentrations of dissolved organic carbon were observed in warmer soils in temperate (Hopkins et al. 2012) and tropical forests (Nottingham et al. 2015). Thus, higher Hg^{2+} concentrations might be expected in runoff as a result of soil warming because of the strong binding of Hg^{2+} with dissolved organic matter (Dittman et al. 2010). Measurements are needed to quantify the magnitude of changes in soil Hg retention due to expected changes in climate for forest ecosystems (Obrist et al. 2018).

From 1980 to 2012, global average air temperature increased by 0.85 °C and the trend is projected to continue over the next century (IPCC 2014). Climate change is also expected to exacerbate the intensity and frequency of climatic disturbances. For example, while mean annual rainfall is expected to increase in many regions, drought occurrence and duration are projected to increase as well (Sheffield and Wood 2008). Ice storms in winter are a common type of extreme event that occurs when moisture-rich warm air overrides subfreezing air at ground level and this event is projected to increase in the future (Hayhoe et al. 2007; Cheng et al. 2011). Direct impacts of ice storms include branch and canopy loss and a reduction in photosynthesis in the following growing season

(Rustad and Campbell 2012) that enhances solar heating in the soil surface and increases the quantity of precipitation passing through the canopy gaps in the following growing season. However, studies have rarely reported the changes in soil evasion and other Hg fluxes in forests under warmed temperatures, droughts, or ice storm events.

We took advantage of three plot-level climate-change manipulation experiments at the Hubbard Brook Experimental Forest, New Hampshire, USA: the Climate Change Across Seasons Experiment, which includes soil warming in the growing season and soil freeze-thaw treatments in winter, a throughfall exclusion experiment to simulate drought and decreases in soil moisture, and a simulated ice storm study. The main objective was to compare the fluxes of Hg in litterfall, throughfall, and soil drainage water and soil Hg^0 evasion among these climate-change manipulation studies. We hypothesized that climate disturbances that result in warmer or wetter soils would stimulate Hg^0 evasion and leaching, whereas drought would have the opposite effect. Ice storm events would be expected to reduce Hg fluxes in litterfall and throughfall during the canopy recovery period. We also evaluated the combined effect of these changes on soil Hg retention.

Materials and methods

Site description

This research was conducted at experimental plots associated with three climate change manipulation experiments located at the Hubbard Brook Experimental Forest in the White Mountain National Forest in Central New Hampshire, USA. The annual mean air temperature ranges from − 9 °C in January to 19 °C in July. The annual precipitation averages 1500 mm (Green et al. 2018). From 1955 to 2015, average annual air temperature warmed by ∼ 1.4 °C and average annual precipitation increased by 300 mm (Bailey et al. 2016). Soils are predominantly Haplorthods developed in glacial drift (Gosz et al. 1976; Vadeboncoeur et al. 2014). Rates of total atmospheric Hg deposition from 2009 to 2011 was estimated to be 22 µg m^{-2} year^{-1} in this region, using data for wet Hg deposition from the National Atmospheric Deposition Program Mercury Deposition Network and estimates

of dry Hg deposition from 2009 to 2011 (Yu et al. 2014).

The soil warming, soil warming + freeze-thaw (Templer et al. 2017) and drought experiments (Jennings et al. 2017) are co-located and share two control plots (43°56′44.2″N, 71°42′03.9″W) at an elevation of 259 m. Plots are dominated by red maple (*Acer rubrum* L.), making up approximately 63% of the total basal area, with American beech (*Fagus grandifolia* Ehrh.) dominating the understory (Templer et al. 2017). The simulated ice storm experiment (Rustad and Campbell 2012; Campbell et al. 2016) is ∼ 8 km away (43°56′12.9″N, 71°46′23.4″W) from the two other experiments at an elevation of 510 m. Ice storm plots are dominated by sugar maple (*Acer saccharum* L.) with an understory of mostly American beech. The manipulated plots were chosen to have similar species composition and total basal area as the control plots.

To examine the effects of soil warming in the growing season and soil freeze-thaw cycles in winter, three plots were selected (each 11 m × 13.5 m): one control plot, one plot with soils warmed by ∼ 5 °C via heating cables during the growing season (warming), and one plot warmed in the growing season and also subjected to four 3-day freezing episodes induced by removing snow by shoveling, separated by 3 days of soil warming (warming + freeze-thaw cycles). These treatments had been applied for 4 years (since December 2013) at the time of our study.

To examine the effect of drought, one plot was selected from the drought experiment (15 m × 15 m) in which ∼ 50% of throughfall was removed by placing gutters 2 m above the ground to cover 50% of the surface area in spring 2015. The treatment was designed to simulate a one-in-a-century drought event. This treatment had been applied for 2 years at the time of our study. An analysis of the treatment effect compared to the 120-year interpolated precipitation data from Parameter-elevation Regressions on Independent Slopes Model confirmed that both treatment years fell below the first percentile of annual precipitation.

To examine the effect of ice storm events, we selected two plots (each 20 m × 30 m, 10 m apart) from the simulated ice storm experiment: one control plot and one high-ice plot, which received 0.75 inches of glaze ice as one event in February 2016, one and a half

years prior to our study (https://hubbardbrook.oncell.com/en/ice-storm-experiment-ise-134482.html).

Measuring soil Hg^0 evasion

Soil Hg^0 evasion was measured continuously for 24–48 h at the center of each of the six plots. Because only a single instrument and one chamber system was available, measurements were conducted sequentially from plot to plot in spring (May 31–June 12), summer (July 28–August 10), and fall (September 29–October 9) in 2017. Measurements were made using a dynamic flux chamber connected to a Tekran 2537A mercury vapor analyzer with a Tekran 1110 two-port controlling unit powered by a generator (Figure S1, Supporting Information). Chambers were placed on-site 24 h prior to the actual measurement to allow the chamber to seal with the soil surface. All the measurements were performed only on sunny days with leaf-litter present to mimic the original environment. In the drought plot, we measured Hg^0 evasion at two locations: one under a gutter and another between two gutters, to capture variability in rainfall exclusion.

We used a 4.32 L rectangular quartz chamber with a height of 0.16 m and a footprint of 0.027 m^2 (0.18 × 0.15 m). Quartz transmits the full spectrum of solar radiation, whereas polycarbonate chambers reflect UV frequencies that influence soil Hg^0 evasion (Moore and Carpi 2005; Bahlmann et al. 2006). Quartz also has a lower potential for Hg^0 absorption (Ci et al. 2016a) and is thus preferred for measuring low rates of Hg^0 evasion from soils. This chamber has eight inlet holes with two holes on each of the four sides (6 mm in diameter; 0.06 m above the surface) and one outlet hole (13.5 mm in diameter) at the center of the top of the chamber. The inlet sampling tube was placed outside the chamber at the same height (0.06 m above the surface) as the inlet holes on the flux chamber. The outlet sampling tube was connected to the outlet hole on the top of the flux chamber. Concentrations of Hg^0 in both the inlet and outlet air were measured alternately twice every 20 min via a valve unit using the two-port controlling unit. Soil Hg^0 evasion was calculated using the following equation:

$$F = (C_{inlet} - C_{outlet}) \times Q \times A^{-1} \qquad (1)$$

where F is soil Hg^0 evasion (ng m^{-2} h^{-1}), C_{inlet} and C_{outlet} are the concentration of Hg^0 inside the flux chamber and in the ambient air (ng m^{-3}), Q is the flow rate of air through the flux chamber (L min^{-1}), and A is the surface area of soil exposed in the chamber (m^2). In this study, Q was 4.4 L min^{-1} and A was 0.027 m^2.

Prior to use, quartz chambers and Teflon tubing were soaked for 24 h in 10% nitric acid, rinsed three times with 18.2 MΩcm Milli-Q water, allowed to dry in a clean room, and then double-bagged with zipper-seal bags. Plastic screws were soaked for 24 h in 10% HCl, rinsed three times with deionized water, and double-bagged with zipper-seal bags. The Tekran 2537A Hg vapor analyzer was calibrated every 12 h with a permeation Hg source, and check standards were run every 6 h. The Hg recovery rate was 98 ± 5%.

Solar radiation on the soil surface (kW m^{-2}), soil temperature (°C) and volumetric soil water content (%) at 2 cm soil depth were measured at 1-min intervals. In the soil warming plots, soil moisture and temperature data were acquired from thermistors and soil moisture probes installed at 0–5 cm depth (model CS616, Campbell Scientific, Logan, UT, USA).

Collection of leaf litterfall, throughfall, soil, and soil solution

Fresh leaf litterfall samples were collected from the soil surface using clean gloves on October 28, 2017. We collected litterfall samples from the dominant species in three replicate locations per plot. All samples were immediately double-bagged in zipper-seal bags, stored on ice during transport, and frozen in the laboratory until they could be analyzed.

Throughfall and open precipitation samples were collected with two replicates in each plot monthly from June to October in 2017 using glass bottles protected from sunlight within a PVC tube for Hg analysis, with one person dedicated to touching the collecting equipment with clean gloves (USEPA 1996). Before the actual deployment, glass funnels, tubing, and glass bottles were soaked for 24 h in 10% nitric acid, rinsed three times with 18.2 M cm Milli-Q water, dried in a clean room, and double-bagged using zipper-seal bags. Glass bottles were stored filled with trace metal grade hydrochloric acid until deployment. The collecting system consisted of a glass funnel

connected to two 500 mL glass bottles via perfluoroalkoxy tubing and styrene-ethylene-butadiene-styrene block polymer tubing with a loop as a vapor lock. Glass wool was placed in the glass funnels to prevent twigs, debris and insects entering through the tubing. Each glass bottle, tubing and glass wool was replaced monthly. Glass bottles with throughfall samples were double-bagged in the field and stored at 4 °C in the laboratory until analysis.

We collected and analyzed throughfall samples in the two control plots only. We did not collect throughfall in treatment plots because we assumed soil warming or freeze-thaw cycles would have little impact on leaf area, although this precluded detection of changes in throughfall Hg concentrations due to deposition on leaf surfaces. We collected open precipitation samples near the simulated ice storm plot.

Soil samples were collected at three replicate locations in each of the six plots in September 2017. We used cleaned split corers in the drought and ice storm plots, and a cleaned plastic knife in the soil warming plots to avoid damage to the heating cables. The corers and the knife were washed with DI water between samples to avoid cross-contamination. Soil samples from organic (Oea) and mineral horizons were collected and bagged in the field. Samples were stored at 4 °C until analysis.

We acquired drainage water samples in the two ice storm plots (control and simulated ice storm) using installed tension lysimeters at soil B horizon pumped into glass bottles from April to June and August in 2017. Unfortunately, soil drainage water samples were utilized for other analyses in the months of July, September and October, so sample was not available for Hg analysis.

Laboratory analyses

Soil samples were sieved through a 0.5 mm stainless steel sieve to acquire homogenized fine soils. Litterfall and processed soil samples were freeze-dried to constant mass at − 80 °C and 7 Pa, using FreeZone Plus 6 (Labconco, Kansas City, MO). Dried litterfall samples were ground using a Freeze Mill (Metuchen, NJ). All samples were analyzed for Hg concentration using thermal decomposition, catalytic conversion, amalgamation, and atomic absorption spectrophotometry (USEPA 1998), using a Milestone DMA 80 direct

Hg analyzer (Shelton, CT) (Yang et al. 2017). Subsamples of $\sim$ 50 mg for soil and $\sim$ 100 mg for leaf litterfall were weighed into nickel boats and autoloaded into the instrument. Aluminum oxide was added to each tissue sample to ensure that the samples were fully oxidized.

Before running tissue samples, we analyzed two blanks, two primers (NIST 1944, waterway sediment, $\sim$ 10 mg, 3400 ± 340 ng g^{-1}), two continuing calibration verification samples (NIST DORM-2, dogfish muscle, $\sim$ 50 mg, 410 ± 41 ng g^{-1}), two quality control samples (NIST 2976 mussel tissue, $\sim$ 50 mg, 61 ± 6 ng g^{-1}, Gaithersburg, MD, USA), and one method blank sample (with aluminum oxide). We did not proceed with sample analysis unless the Hg recovery values of these quality control samples were within 10% of the certified values. After every 10 samples, we ran continuing calibration verifications (NIST DORM-2) and continuing calibration blanks. A sample batch consisted of a method blank, a quality control sample, a duplicate, a matrix spike and a matrix spike duplicate. The matrix spike was one actual tissue sample spiked with the standard reference material (NIST DORM-2). The average Hg recovery was 99% (n = 6, rsd = 5%) of NIST 1944, 105% (n = 12, rsd = 3%) of DORM-2, 103% (n = 8, rsd = 4%) of NIST 2976 and 102% (n = 8, rsd = 5%) of the matrix spike, which were all within the acceptable range of values.

Throughfall, open precipitation, and soil drainage water samples were analyzed for total Hg concentrations via oxidation with bromine chloride for a minimum of 24 h, purge and trap, and cold vapor atomic fluorescence spectroscopy (USEPA 2002) on a Tekran 2600 automated total Hg analyzer. The method detection limit was 0.2 ng L^{-1}. Both field blanks (n = 30) of the Hg sampling trains and laboratory blanks (n = 15) had Hg concentrations below the detection limit, and sample-train standard spikes (5 ng L^{-1}) had recoveries of 102% (n = 12, rsd = 7%).

Analyzing soil Hg^0 evasion and Hg concentrations in litterfall, soil and drainage water

To explore relationships between meteorological variables and soil Hg^0 evasion, linear regression analysis was used with hourly data from each plot across each season. To explore the differences in Hg concentrations in leaf litterfall associated with climate

effects (6 plots) for each tree species, a one-way ANOVA with Tukey's Honestly Significant Difference (HSD) was used with three replicates sampled in each plot. Differences in litterfall Hg concentrations among tree species were also tested using one-way ANOVA using three replicates within each plot and blocked by plots.

Two-way ANOVA with Tukey's HSD was used to characterize the effects of soil horizon (two levels) and climate disturbance effects (6 manipulation plots).

Concentrations were log-transformed in both analyses to meet the assumption of normality of the residuals. Statistical analyses were conducted in SAS 9.4 (SAS Institute, Inc. 2013).

Estimate of annual soil Hg retention

To estimate annual litterfall Hg fluxes, we multiplied Hg concentrations by the measured annual litterfall mass of each tree species. For the less abundant tree species that we did not sample, we used the average concentration of our measured species as the Hg concentration and multiplied by the mass of their annual litterfall. Leaf litterfall was collected using five litter traps (one at the center and four near the corners) in the plots from September to November in 2017. We also calculated the Hg in falling twigs and branches during the icing event using the reported mass of samples collected in traps in 2016 (Driscoll et al. 2016) multiplied by the reported Hg concentrations in tree woody materials at the Hubbard Brook Experimental Forest (Yang et al. 2018).

To estimate throughfall Hg fluxes, we used monthly precipitation volumes measured from standard rain gauges (one near the simulated ice-storm plots and one near the drought and soil warming plots) multiplied by throughfall Hg concentrations. For the non-growing season (November to May), we used the average of our measured Hg concentrations in open precipitation. For the leaf-on season (June to October), we measured throughfall concentrations in the two control plots. We used a weighted average concentration of throughfall and open precipitation, based on a 2% canopy opening for the two control plots and a 7% canopy opening for the simulated ice storm plot (Robert T. Fahey, University of Connecticut, unpublished LiDAR data).

To estimate the annual flux of soil Hg^0 evasion, we used the average of the spring, summer, and fall measurements, and assumed that winter fluxes

accounted for only 5% additional flux based on measurements at the Huntington Forest in New York (Choi and Holsen. 2009).

To estimate the annual export of dissolved Hg in the two plots in the simulated ice storm experiments, we multiplied our Hg concentrations in drainage water by the estimated soil water discharge from the Bhs horizon for each month. For the months with insufficient volume for analysis, we used the average of our measured Hg concentrations in the other months. The annual soil water discharge was estimated to be 966 mm with a range of 27–252 mm across months (Habibollah Fakhraei, Syracuse University, personal communication), using the BROOK90 hydrological model (Federer 2002), applied to the Hubbard Brook watersheds.

The annual soil Hg retention in each plot compared the litterfall and throughfall Hg inputs to the outputs in soil Hg evasion and Hg runoff in drainage water.

Results

Soil Hg^0 evasion and meteorological variables

Soil Hg^0 evasion was altered in climate manipulation experiments (Table 1). The warmed plot and the warming + freeze-thaw plot had 28% and 32% higher average rates of Hg^0 evasion, respectively, than the control plot in June, 36% and 40% higher in August and 26% and 30% higher in October (Fig. 1). Both of the treatments involving warming resulted in an increase of ~ 5 °C in soil temperature (Fig. 1), but neither solar radiation (Fig. 1) nor soil moisture ($\sim 24\%$ in June, $\sim 18\%$ in August and $\sim 15\%$ in October) differed by treatment.

In the second growing season after the simulated ice storm, soil Hg^0 evasion was 31% higher in June, 48% higher in August and 28% higher in October compared to the control plot (Fig. 2). The simulated ice storm resulted in an increase in solar radiation of 0.07 kW m^{-2} in June, 0.14 kW m^{-2} in August and 0.06 kW m^{-2} in October (Fig. 2), but neither soil temperature (~ 13 °C in June, ~ 16 °C in August, ~ 12 °C in October) nor soil moisture ($\sim 37\%$ in June, $\sim 33\%$ in August, $\sim 28\%$ in October) differed by treatment.

In contrast to the ice storm and soil temperature treatments, the drought treatment reduced rates of soil

Table 1 Soil Hg^0 evasion at different climate change manipulation and control plots for three seasons at the Hubbard Brook Experimental Forest

Study site	Experimental plots	Average hourly surface-air gas Hg fluxes $\pm$ SD (ng m^{-2} h^{-1})		
		Spring (June)	Summer (August)	Fall (October)
Climate change across seasons experiment and throughfall exclusion experiment	Control	1.06 ± 0.97	1.48 ± 1.18	0.84 ± 0.63
	Warming	1.36 ± 1.19	2.02 ± 1.35	1.06 ± 0.66
	Warming and freeze–thaw cycles	1.40 ± 1.23	2.07 ± 1.33	1.09 ± 0.74
	Drought between gutters	0.84 ± 0.81	1.19 ± 0.83	0.68 ± 0.44
	Drought under a gutter	0.82 ± 0.68	1.14 ± 0.70	0.67 ± 0.47
Simulated ice storm experiment	Control	1.30 ± 1.17	1.63 ± 1.09	1.04 ± 0.73
	Simulated ice storm	1.70 ± 1.32	2.40 ± 1.53	1.34 ± 1.02

SD represented standard deviation of 24 h within a day

Hg^0 evasion by 20–22% relative to the control in all 3 months of study (Fig. 3). There was little difference in soil Hg^0 evasion measured in chambers placed under a gutter or between gutters (1–4% varied across seasons). The drought treatments resulted in a decrease of 1%-4% in soil moisture (Fig. 3), but neither solar radiation (Fig. 3) nor soil temperature ($\sim$ 12 °C in June, $\sim$ 19 °C in August and $\sim$ 14 °C in October) differed by treatment.

Not surprisingly, soil Hg^0 evasion measurements varied diurnally and across seasons, consistent with patterns of soil temperature and solar radiation. Hourly Hg^0 evasion was positively correlated with surface soil temperature ($p \leq 0.03$) and solar radiation ($p < 0.001$) across all plots and seasons using hourly measurements in simple linear regressions. Hourly Hg^0 evasion was not correlated with soil moisture across all plots and seasons ($p \geq 0.25$).

Concentrations of Hg in litterfall, soil, throughfall and drainage water

Mercury concentrations in litter varied by species, with higher litterfall Hg concentrations in American beech (48–55 ng g^{-1}) than red maple, sugar maple, and yellow birch (25–40 ng g^{-1}; $p < 0.001$ across all plots; Fig. 4). Concentrations of litterfall Hg for yellow birch increased 19% in the warmed plot (40.7 $\pm$ 1.1 ng g^{-1}) and decreased 26% in the drought plot (25.1 $\pm$ 1.3 ng g^{-1}) compared to the control plot (34.1 $\pm$ 0.8 ng g^{-1}, $p < 0.001$). Concentrations of litterfall Hg for American beech, red maple and sugar maple did not respond consistently to warming or drought ($p \geq 0.13$). In the ice

storm experiment, litterfall Hg concentrations for American beech were 8% lower in the ice storm plot (51.1 $\pm$ 1.4 ng g^{-1}) than the control plot (55.5 $\pm$ 0.8 ng g^{-1}, $p = 0.06$). Concentrations of Hg in litterfall for yellow birch, red maple and sugar maple did not respond significantly to the simulated ice storm ($p \geq 0.11$).

Concentrations of soil Hg were consistently higher in the organic (0.25 $\pm$ 0.01 mg kg^{-1}) than the mineral horizon (0.18 $\pm$ 0.01 mg kg^{-1}) across all plots ($p < 0.001$; Figure S2, Supporting Information). Concentrations of soil Hg did not differ in the climate manipulation plots compared to the control plots either in the organic or mineral horizon ($p \geq 0.12$).

Concentrations of throughfall Hg were similar in the two control plots, averaging 4.1 $\pm$ 1.6 and 5.1 $\pm$ 0.9 ng L^{-1} from June to October. Concentrations of Hg in throughfall were 1.5–2.5 times higher than those for open precipitation (average of 2.6 $\pm$ 0.6 ng L^{-1}) from June to October.

In the second growing season after the ice storm experiment, concentrations of Hg in drainage water from lysimeters in the ice storm plot (2.9 $\pm$ 1.4 ng L^{-1}) were 2–2.9 times higher than those in the control plot (1.2 $\pm$ 0.6 ng L^{-1}).

Fluxes of Hg

Mercury deposition in litterfall was affected by the simulated ice storm, drought, and soil temperature experiments due to changes in both litterfall mass and Hg concentration. In the second year after the simulated ice storm, leaf litterfall mass was 15%
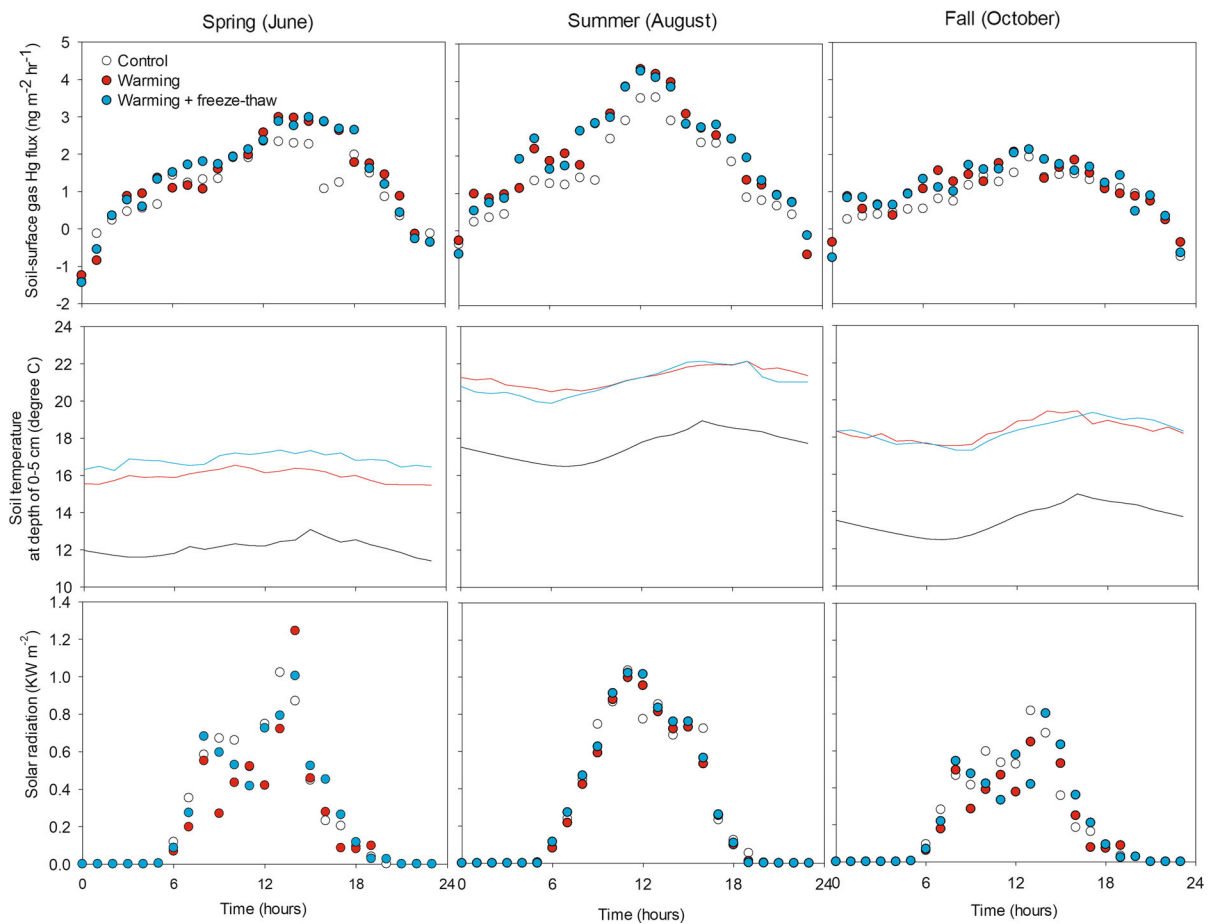
Fig. 1 Soil Hg^0 evasion and soil temperature and solar radiation at soil warming, soil warming + freeze–thaw cycles, and control plots across the three sampling dates

lower and leaf litterfall Hg concentration was 8% lower, resulting in a 11% reduction of leaf litterfall Hg flux in the treatment than in the control plot (Fig. 5). Decreases in total leaf litter mass averaged 25%, except for American beech, which decreased by only 5%. However, the input of woody material in the first year after the treatment increased by 670 g m^{-2} (4 µg Hg m^{-2}), and thus total litterfall Hg deposition was 23% higher in the simulated ice storm plot than the control. The drought treatment decreased litterfall mass by 3% and litterfall Hg flux by 5% compared to the control plot. Soil warming increased leaf litterfall mass by 14% and litterfall Hg flux by 7% compared to the control plot. Soil warming and freeze-thaw resulted in a reduction of 8% in litterfall mass and an 18% reduction in litterfall Hg.

Mercury deposition in throughfall reflected treatment effects on precipitation volume. Throughfall Hg fluxes in the drought plot were assumed to be 50% of those in the control, because of the removal of half of the throughfall by the gutters. The simulated ice storm had little effect on throughfall volume (2% increase) or Hg flux (1% decrease), which was not surprising as there was only a 5% reduction in canopy cover (Fig. 5).

Annual Hg output via soil evasion was increased by the simulated ice storm and by soil warming but decreased by drought. Annual soil Hg^0 evasion was 37% higher in the simulated ice storm plot, 31% higher in the warming plot and 35% higher in the soil warming + freeze-thaw plot than in the respective controls (Fig. 5). The drought plot decreased Hg^0 evasion by 21% compared to the control plot.
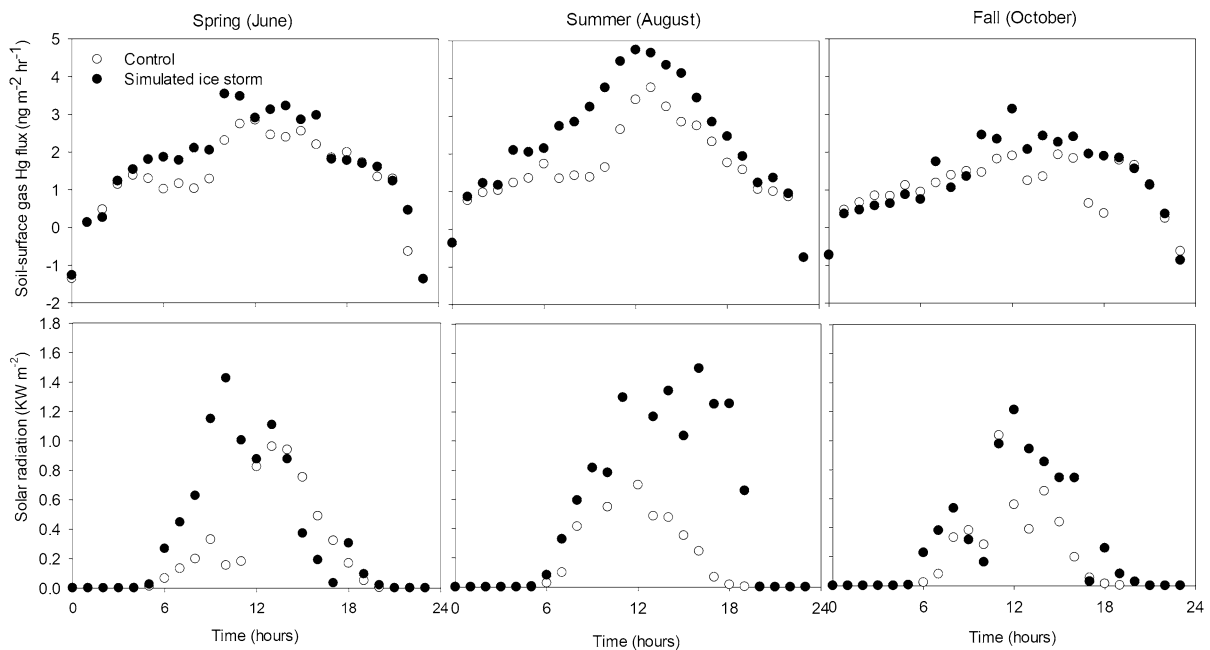
Fig. 2 Soil Hg^0 evasion was stimulated following a simulated ice storm at three sampling dates. Solar radiation was also higher in the plot with the simulated ice storm

Annual Hg output via soil drainage water was measured only in the two plots at the simulated ice storm sites, where it was 151% higher in the simulated ice storm plot than in the control, assuming the discharge rate was the same.

Comparing Hg inputs to the soil (litterfall and throughfall) with Hg outputs (soil evasion), soil Hg retention was 16–60% lower at the soil warming (6.4 µg m^{-2} year^{-1}), soil warming + freeze-thaw (3.4 µg m^{-2} year^{-1}), and drought plots (6.8 µg m^{-2} year^{-1}) than in the control (8.1 µg m^{-2} year^{-1}). In the simulated ice storm plot, where we estimated Hg in woody materials as an additional input and Hg leaching as an additional output, soil Hg retention was 41% lower (3.9 µg m^{-2} year^{-1}) than in the control (6.6 µg m^{-2} year^{-1}).

Discussions

### Magnitudes of input and output Hg fluxes in undisturbed plots

In our two undisturbed plots, litterfall Hg fluxes (~ 11.5 µg m^{-2} year^{-1}) were similar to those reported for 23 hardwood stands in the eastern USA

(average of 11.7 µg m^{-2} year^{-1}) (Risch et al. 2017). Our throughfall Hg fluxes (~ 4.7 µg m^{-2} year^{-1}) were comparable to those reported for hardwood stands at Huntington Forest (6.9 µg m^{-2} year^{-1}; Blackwell et al. 2014) and Sunday Lake Watershed (7.4 µg m^{-2} year^{-1}; Demers et al. 2007) in New York. Inputs of Hg to soil by litterfall that exceed values in throughfall have been reported in northern mixed-hardwood forests in Vermont and Michigan (Rea et al. 2002) and in a study of 92 forested sites across North America (Wright et al. 2016).

The soil Hg^0 evasion rates ranged from 0.8 to 1.6 ng m^{-2} h^{-1} over three measurement dates, and were similar to the reported values in those three seasons for hardwood forests in Sweden (0.9–1.9 ng m^{-2} h^{-1}) (Schroeder et al. 1989), various types of forests in Nova Scotia in Canada (− 0.4 to 2.2 ng m^{-2} h^{-1}) (Schroeder et al. 2005), hardwood forests in Michigan (− 0.2 to 2.4 ng m^{-2} h^{-1}) (Zhang et al. 2001), upslope mixed forests in Connecticut (0.9–3.0 ng m^{-2} h^{-1}) (Sigler and Lee 2006) and hardwood forests in New York (0.8–1.6 ng m^{-2} h^{-1}) (Choi and Holsen 2009). Soils at these sites had soil Hg concentrations similar to ours, ranging from 0.1 to 0.4 µg g^{-1}.

Leaching losses of Hg from the mineral soils (1.3 µg m^{-2} year^{-1}) were comparable to the values
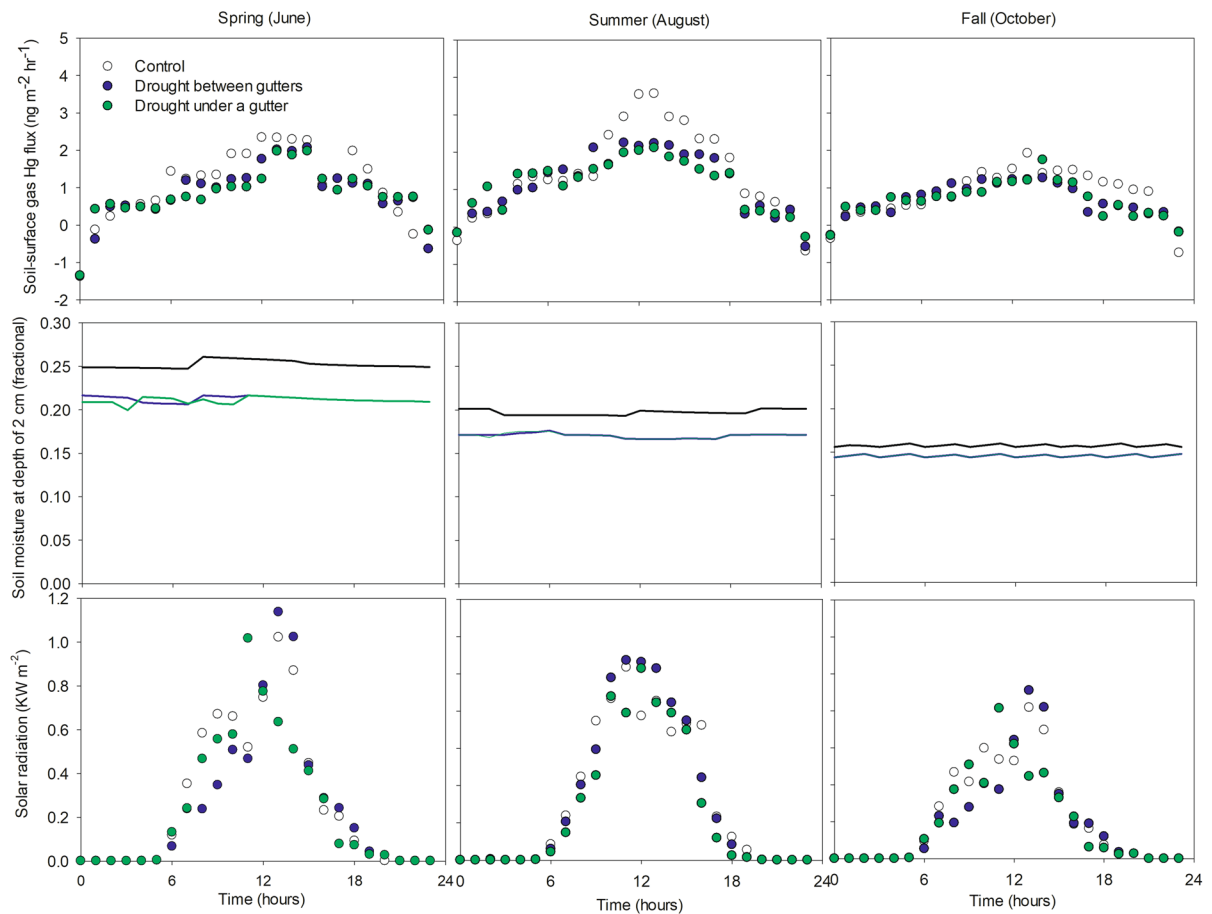
Fig. 3 Soil Hg^0 evasion was suppressed by drought treatment at three sampling dates
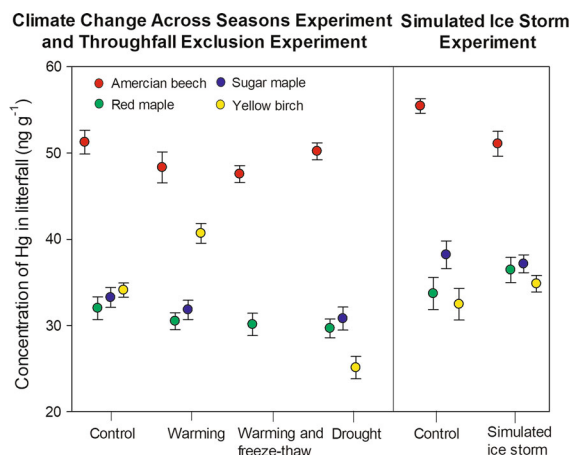
Fig. 4 Mean concentrations of Hg in leaf litterfall in major species at different manipulation plots. Error bars represent the SE of three replicate samples in a plot. The soil warming and warming + freeze-thaw plot had only two of the four species

reported for hardwood forests in Minnesota (0.8 μg m^{-2} year^{-1}) (Kolka et al. 2001) and the Adirondacks of New York in the USA (1.1 μg m^{-2} year^{-1}) (Wang 2012) and a boreal forest in Sweden (1.3 μg m^{-2} year^{-1}) (Osterwalder et al. 2017). We found that the amount of Hg leached was an order of magnitude smaller than losses by soil Hg^0 evasion in the undisturbed plot at the simulated ice storm site (Fig. 5). Runoff or erosion of Hg was not measured in this study, but other studies suggest that the combined Hg output including runoff, soil leaching and soil erosion is low, e.g., 2.0 μg m^{-2} year^{-1} in New Brunswick Forests in Canada (Nasr and Arp 2015), 2.2 μg m^{-2} year^{-1} in Minnesota (Kolka et al. 2001) and 1.7 μg m^{-2} year^{-1} in the Adirondack Region in New York, USA (Wang 2012).

We found that forest soils served as a Hg net sink in undisturbed control plots, because inputs of Hg via litterfall and throughfall deposition exceeded Hg
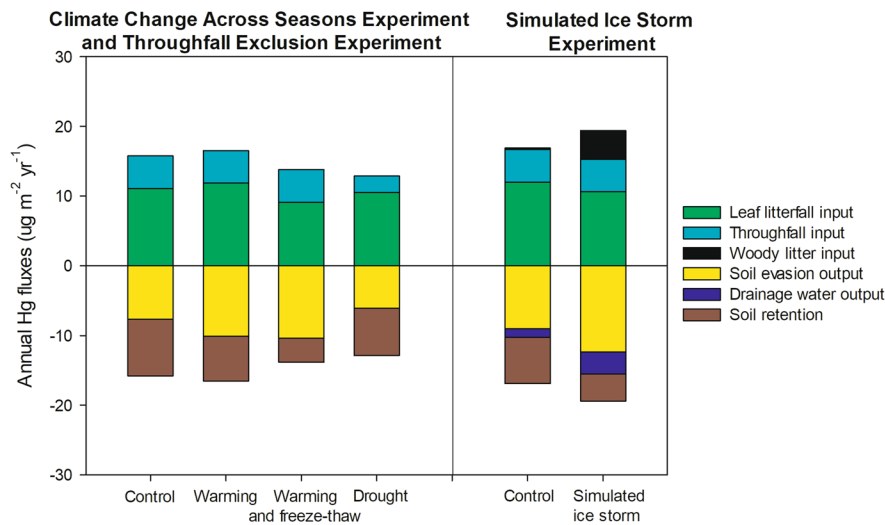
Fig. 5 Measured annual Hg inputs (litterfall and throughfall) and outputs (soil evasion and drainage water) for experiments depicting three climate change manipulations in northern hardwood at the Hubbard Brook Experimental Forest, NH. Soil Hg retention was calculated by difference. Input of Hg in twigs and branches and output of Hg via soil water discharge were measured only in the simulated ice storm plots; soil Hg retention was overestimated in the other plots by the amount of Hg in the drainage water and underestimated by the amount of Hg in woody litter

outputs via evasion and documented runoff. This pattern is consistent with studies in a hardwood-peatland watershed in Minnesota (20 μg m^{-2} year^{-1}, Grigal et al. 2000), a forested catchment in southeast Norway (6.9 μg m^{-2} year^{-1}, Larssen et al. 2008), and northern hardwood (15.5 μg m^{-2} year^{-1}) and conifer stands (34.6 μg m^{-2} year^{-1}) at the Huntington Forest in New York (Blackwell et al. 2014). The input of Hg via litterfall and throughfall is due to the capturing of atmospheric Hg by the forest canopy (St. Louis et al. 2001; Ericksen et al. 2003; Jiskra et al. 2018). The limited Hg output from soil discharge water (Różański et al. 2016) and evasion (Yang et al. 2007) are likely due to the binding of Hg^{2+} by soil organic matter.

Effects of changing climate on litterfall and throughfall Hg

Changes in litterfall Hg fluxes in the warming and drought plots compared to the control plots are mainly due to the changes of litterfall Hg concentrations rather than differences in litterfall mass. The higher litterfall Hg concentrations for yellow birch in the warmed plot may be due to a higher rate of Hg^0 uptake via stomata in response to the increases in soil temperature. Experimental increases in soil temperature have been reported to increase root hydraulic conductivity (Cochard et al. 2000; Wieser et al. 2015), which would allow greater transpiration and stomatal conductance (Wieser et al. 2015; Juice et al. 2016). Higher stomatal conductance in hardwood species was found to facilitate foliar uptake of atmospheric Hg^0 in a greenhouse experiment (Millhollen et al. 2006). Conversely, the lower Hg concentrations of yellow birch leaf litter in the drought plot might be due to drought-induced stomatal closure and reduced foliar uptake of Hg^0. Lower Hg concentrations in foliage in a dry year in comparison to a wet year in the Adirondacks of New York was attributed to lower stomatal conductance (Blackwell et al. 2014). Although Hg concentrations were altered under warming and drought treatments for yellow birch leaf litter, changes in annual litterfall Hg flux were small ($< 10\%$) because of the small proportion of yellow birch litter mass (21% of the total litterfall mass in our plots). Forests that having a larger basal area of yellow birch would likely to have greater changes in litterfall Hg fluxes. It is not clear why other hardwood species were less sensitive to the soil warming and drought experiments. At a study of four sites in northeastern America, yellow birch was found to have higher wood Hg concentrations than American beech, sugar maple and red maple, but not the greatest foliar Hg concentrations (Yang et al. 2018). Wood is the tissue that

stores the greatest amounts of Hg (Yang et al. 2018), which suggests that yellow birch has greater Hg uptake or lower Hg losses that the other hardwood species.

Reduced leaf litterfall mass and increased woody materials found in our simulated ice storm plot was consistent with other studies. A decrease in leaf litter mass due to canopy reduction by an ice storm event has been reported in a bamboo forest in China (Ge et al. 2014). The large input of tree woody materials after the manipulated ice storm event is consistent with measurements in conifer stands in China (Xu et al. 2016) and in an earlier simulated ice-storm near our plots at Hubbard Brook in New Hampshire in U.S (Rustad and Campbell 2012).

Throughfall inputs of Hg were similar in the simulated ice storm and the control plot. Similar Hg fluxes between throughfall and open precipitation have also been reported in hardwood stands at the Huntington forests (6.9 and 6.7 μg m^{-2} $year^{-1}$) (Blackwell et al. 2014) and at Whiteface Mountain (4.5 and 4.2 μg m^{-2} $year^{-1}$) (Gerson et al. 2017) in New York. These observations suggest that dry deposition of Hg^{2+} to foliar surfaces and subsequent leaching to the forest floor is a minor pathway of Hg inputs in remote hardwood forests. However, in conifer stands, throughfall Hg concentrations can be three times higher than values in open areas, due to the greater leaf area index of conifer stands compared to hardwoods (Demers et al. 2007; Blackwell et al. 2014).

Effects of changing climate on soil Hg^0 evasion and Hg^{2+} leaching

The diurnal pattern of soil Hg^0 evasion was driven mainly by the diurnal variation in soil temperature and solar radiation. The observed strong correlation between hourly Hg^0 evasion and soil temperature on a diurnal basis is consistent with other studies of soil Hg^0 evasion (Gabriel et al. 2006; Park et al. 2013). The poor correlation between hourly Hg^0 evasion and soil moisture in this study is not surprising given the lack of variation in soil moisture (coefficient of variation $< 3\%$). This poor relationship has also been reported in upslope mixed forests in Connecticut where variation in soil moisture was $< 10\%$ during the field campaigns (Sigler and Lee 2006).

Differences in soil Hg^0 evasion due to treatment could be explained by differences in meteorological conditions resulting from the treatments. Increased soil Hg^0 evasion under soil warming was likely due to increases in soil temperature. The lower soil Hg^0 evasion in the drought plot than the control plot may be explained by reductions in upward transport of Hg by capillary action (Briggs and Gustin 2013). Precipitation has increased by 300 mm from 1955 to 2015 at the Hubbard Brook Experimental Forest (Bailey 2016). Thus, we might expect increased Hg^0 evasion from soils due to a wetter climate in the future. The higher soil Hg^0 evasion in the simulated ice storm is likely explained by increases in solar radiation due to canopy gaps; increases in soil temperature were small (averaging ~ 0.6 °C during our measurements and ~ 0.3 °C for the year according to the installed thermistors). Solar radiation affects Hg^0 evasion by reducing Hg^{2+} to Hg^0 and releasing soil-bound Hg to the air (Zhang and Lindberg 1999; Gustin et al. 2002; Park et al. 2013). After clear cutting, soil Hg^0 evasion was reported to increase from -0.7 to 9 ng m^{-2} h^{-1} in hardwood forests in New York and from 0.3 to 21 m^{-2} h^{-1} in Brazil (Carpi et al. 2014), and from -7.5 to 2 ng m^{-2} h^{-1} in mixed forests in Minnesota (Mazur et al. 2014). It is not surprising that we observed smaller effects on Hg^0 evasion from the simulated ice storm, because damage to the forest canopy was small (5% reduction of canopy cover in the second growing season) compared to the complete removal of the overstory associated with forest harvesting.

Differences in soil Hg concentrations were not significant across our plots, but we estimated the magnitude of differences in soil Hg evasion that could be due to the variation in soil Hg across the plots. We applied the equation developed by Eckley et al. (2016): soil Hg^0 evasion (ng m^{-2} h^{-1}) = soil THg (μg g^{-1}) $\times$ 0.54 (mg m^{-2} h^{-1}) + 1.3 (ng m^{-2} h^{-1}). The coefficient of variation of estimated soil Hg^0 evasion across the six plots was only 1.2%, and thus the variation in soil Hg was not likely important to the differences in Hg^0 evasion that we observed. The influence of differences in solar radiation on different days was likely higher, based on the relationships we observed each season between solar radiation and soil Hg^0 evasion. The coefficient of variation of estimated soil Hg^0 evasion due to solar radiation was 7%, but this was less than the actual differences of soil Hg^0 evasion

due to warming (at least 26%, depending on the season) and drought effects (at least 20%). In the simulated ice storm plots, differences in solar radiation were large (coefficient of variation > 56%), due to the opened canopy, and these differences had important effects on soil Hg^0 evasion.

Increases in Hg^{2+} leaching from soils in the simulated ice storm plot were likely due to the mobilization of dissolved organic matter released from soils and the strong binding of Hg^{2+} to dissolved organic matter (Skyllberg et al. 2000; Haitzer et al. 2002; Stoken et al. 2016). Concentrations of dissolved organic carbon were 1.7 times higher in the ice storm plot (average of 9.3 ± 0.7 mg L^{-1} from April to October) than the control plot (average of 5.6 ± 0.8 mg L^{-1}) (unpublished data) presumably due to the large addition of litterfall. Higher rates of litter decomposition and more dissolved organic carbon were observed after a severe ice storm in a conifer stand in China (Xu et al. 2016). Although we did not characterize Hg^{2+} leached under soil warming, Hg^{2+} leaching may have been accelerated there as well, associated with root damage (Sanders-DeMott et al. 2018), as root decomposition is a significant source of Hg to soils (Wang et al. Wang 2012). Soil warming would also be expected to increase decomposition, which would hasten the release of Hg from both roots and aboveground litter.

Conclusions

Forests continue to act as a Hg sink for atmospheric Hg deposition under conditions of soil warming, soil warming combined with soil freeze–thaw cycles, drought, and ice storm disturbance, but with diminished net Hg removal compared to the undisturbed controls. Climate changes such as increases in soil or air temperatures and the frequency and intensity of ice storms are likely to exacerbate Hg pollution by releasing Hg previously sequestered in forest soils. The drought treatment resulted in a decrease in Hg^0 evasion losses, but there was also a greater decrease in litterfall and throughfall Hg input resulting in a decrease in soil Hg retention. Under experimental conditions, we observed that the ice storm treatment increased both inputs and outputs of Hg fluxes more than soil warming or soil warming and freeze-thaw cycles. The impacts of ice storms are likely to be short-lived as the forest canopy recovers from the damage. However, soil warming and a reduced winter snowpack, resulting in greater soil freeze-thaw cycles, would result in a chronic increase in Hg output, which is greater cause for concern over the long term.

References

Bahlmann E, Ebinghaus R, Ruck W (2006) Development and application of a laboratory flux measurement system (LFMS) for the investigation of the kinetics of mercury emissions from soils. J Environ Manag 81(2):114–125

Bailey AS, Campbell JL, Green MB, Rustad L (2016) Long-term trends and foundation datasets at Hubbard Brook Experimental Forest, Woodstock, New Hampshire, USA. U.S. Forest Service, General Technical Report, in preparation, last updated on November 30, 2016. https://hubbardbrook.org/sites/default/files/pictures/HBRF/ScienceLinks/Climate%20WEB.pdf

Blackwell BD, Driscoll CT, Maxwell JA, Holsen TM (2014) Changing climate alters inputs and pathways of mercury deposition to forested ecosystems. Biogeochemistry 119(1–3):215–228

Briggs C, Gustin MS (2013) Building upon the conceptual model for soil mercury flux: evidence of a link between moisture evaporation and Hg evasion. Water Air Soil Pollut 224(10):1744

Bushey JT, Nallana AG, Montesdeoca MR, Driscoll CT (2008) Mercury dynamics of a northern hardwood canopy. Atmos Environ 42(29):6905–6914

Campbell JL, Rustad L, Driscoll CT, Fahey T, Garlick S, Groffman P, Schaberg PG (2016) Evaluating the impacts of extreme events on ecological processes through the lens of an ice storm manipulation experiment. In AGU Fall Meeting Abstracts

Carpi A, Fostier AH, Orta OR, dos Santos JC, Gittings M (2014) Gaseous mercury emissions from soil following forest loss

and land use changes: field experiments in the United States and Brazil. Atmos Environ 96:423–429

Chan HM, Scheuhammer AM, Ferran A, Loupelle C, Holloway J, Weech S (2003) Impacts of mercury on freshwater fish-eating wildlife and humans. Hum Ecol Risk Assess 9(4):867–883

Chen C, Amirbahman A, Fisher N, Harding G, Lamborg C, Nacci D, Taylor D (2008) Methylmercury in marine ecosystems: spatial patterns and processes of production, bioaccumulation, and biomagnification. EcoHealth 5(4):399–408

Cheng CS, Li G, Auld H (2011) Possible impacts of climate change on freezing rain using downscaled future climate scenarios: updated for eastern Canada. Atmos Ocean 49(1):8–21

Choi HD, Holsen TM (2009) Gaseous mercury fluxes from the forest floor of the Adirondacks. Environ Pollut 157(2):592–600

Choi HD, Sharac TJ, Holsen TM (2008) Mercury deposition in the Adirondacks: a comparison between precipitation and throughfall. Atmos Environ 42(8):1818–1827

Ci Z, Zhang X, Yin Y, Chen J, Wang S (2016a) Mercury redox chemistry in waters of the eastern Asian seas: from polluted coast to clean open ocean. Environ Sci Technol 50(5):2371–2380

Ci Z, Peng F, Xue X, Zhang X (2016b) Air–surface exchange of gaseous mercury over permafrost soil: an investigation at a high-altitude (4700 m asl) and remote site in the central Qinghai-Tibet Plateau. Atmos Chem Phys 16(22):14741–14754

Cochard H, Martin R, Gross P, Bogeat-Triboulot MB (2000) Temperature effects on hydraulic conductance and water relations of *Quercus robur* L. J Exp Bot 51(348):1255–1259

Demers JD, Driscoll CT, Fahey TJ, Yavitt JB (2007) Mercury cycling in litter and soil in different forest types in the Adirondack region, New York, USA. Ecol Appl 17(5):1341–1351

Denkenberger JS, Driscoll CT, Branfireun BA, Eckley CS, Cohen M, Selvendiran P (2012) A synthesis of rates and controls on elemental mercury evasion in the Great Lakes Basin. Environ Pollut 161:291–298

Dittman JA, Shanley JB, Driscoll CT, Aiken GR, Chalmers AT, Towse JE, Selvendiran P (2010) Mercury dynamics in relation to dissolved organic carbon concentration and quality during high flow events in three northeastern US streams. Water Resour Res. https://doi.org/10.1111/eip.12846

Driscoll CT, Han YJ, Chen CY, Evers DC, Lambert KF, Holsen TM, Kamman NC, Munson RK (2007) Mercury contamination in forest and freshwater ecosystems in the northeastern United States. Bioscience 57(1):17–28

Driscoll CT, Fakhraei H, Campbell JL, Groffman PM, Fahey TJ, Rustad LE, Likens GE (2016) Response of experimental forest watersheds at the Hubbard Brook Experimental Forest, NH to winter climatic disturbance events. American Geophysical Union Chapman Conference. San Juan, Puerto Rico

Eckley CS, Tate MT, Lin CJ, Gustin M, Dent S, Eagles-Smith C, Lutz MA, Wickland KP, Wang B, Gray JE, Edwards GC (2016) Surface-air mercury fluxes across Western North America: a synthesis of spatial trends and controlling variables. Sci Total Environ 568:651–665

Ericksen JA, Gustin MS, Schorran DE, Johnson DW, Lindberg SE, Coleman JS (2003) Accumulation of atmospheric mercury in forest foliage. Atmos Environ 37(12):1613–1622

Federer CA (2002) BROOK 90: a simulation model for evaporation, soil water, and streamflow. http://www.ecoshift.net/brook/brook90.htm

Gabriel MC, Williamson DG, Zhang H, Brooks S, Lindberg S (2006) Diurnal and seasonal trends in total gaseous mercury flux from three urban ground surfaces. Atmos Environ 40(23):4269–4284

Ge X, Zhou B, Tang Y (2014) Litter production and nutrient dynamic on a Moso bamboo plantation following an extreme disturbance of 2008 ice storm. Adv Meteorol. https://doi.org/10.1155/2014/750865

Gerson JR, Driscoll CT, Demers JD, Sauer AK, Blackwell BD, Montesdeoca MR, Shanley JB, Ross DS (2017) Deposition of mercury in forests across a montane elevation gradient: elevational and seasonal patterns in methylmercury inputs and production. J Geophys Res 122(8):1922–1939

Gosz JR, Likens GE, Bormann FH (1976) Organic matter and nutrient dynamics of the forest and forest floor in the Hubbard Brook Forest. Oecologia 22(4):305–320

Graydon JA, St. Louis VL, Hintelmann H, Lindberg SE, Sandilands KA, Rudd JW, Kelly CA, Tate MT, Krabbenhoft DP, Lehnherr I (2009) Investigation of uptake and retention of atmospheric Hg(II) by boreal forest plants using stable Hg isotopes. Environ Sci Technol 43(13):4960–4966

Green MB, Campbell JL, Yanai RD, Bailey SW, Bailey AS, Grant N, Halm I, Kelsey EP, Rustad LE (2018) Downsizing a long-term precipitation network: using a quantitative approach to inform difficult decisions. PLoS ONE 13(5):e0195966

Grigal DF, Kolka RK, Fleck JA, Nater EA (2000) Mercury budget of an upland-peatland watershed. Biogeochemistry 50(1):95–109

Gustin MS, Biester H, Kim CS (2002) Investigation of the light-enhanced emission of mercury from naturally enriched substrates. Atmos Environ 36(20):3241–3254

Haitzer M, Aiken GR, Ryan JN (2002) Binding of mercury (II) to dissolved organic matter: the role of the mercury-to-DOM concentration ratio. Environ Sci Technol 36(16):3564–3570

Hayhoe K, Wake CP, Huntington TG, Luo L, Schwartz MD, Sheffield J, Wood E, Anderson B, Bradbury J, DeGaetano A, Troy TJ, Wolfe D (2007) Past and future changes in climate and hydrological indicators in the US Northeast. Clim Dyn 28(4):381–407

Haynes KM, Kane ES, Potvin L, Lilleskov EA, Kolka RK, Mitchell CP (2017) Gaseous mercury fluxes in peatlands and the potential influence of climate change. Atmos Environ 154:247–259

Hopkins FM, Torn MS, Trumbore SE (2012) Warming accelerates decomposition of decades-old carbon in forest soils. Proc Natl Acad Sci 109(26):E1753–E1761

IPCC (2014) Climate change 2014: synthesis report. Contribution of Working Groups I, II and III to the Fifth Assessment Report of the Intergovernmental Panel on Climate Change

[Core Writing Team, R.K. Pachauri and L.A. Meyer (eds)]. IPCC, Geneva, Switzerland, pp 151

Jennings K, McIntire C, Coble A, Vandeboncoeur M, Rustad L, Templer P, Absbjornsen H (2017) Tree species' responses to throughfall removal experiments superimposed on a natural drought event in two contrasting humid temperate forests in New Hampshire, USA. In EGU General Assembly Conference Abstracts (Vol. 19, p. 19461)

Jiskra M, Sonke JE, Obrist D, Bieser J, Ebinghaus R, Myhre CL, Pfaffhuber KA, Wängberg I, Kyllönen K, Worthy D, Martin LG (2018) A vegetation control on seasonal variations in global atmospheric mercury concentrations. Nat Geosci 11(4):244

Juice SM, Templer PH, Phillips NG, Ellison AM, Pelini SL (2016) Ecosystem warming increases sap flow rates of northern red oak trees. Ecosphere 7(3):e01221

Kolka RK, Grigal DF, Nater EA, Verry ES (2001) Hydrologic cycling of mercury and organic carbon in a forested upland–bog watershed. Soil Sci Soc Am J 65(3):897–905

Laacouri A, Nater EA, Kolka RK (2013) Distribution and uptake dynamics of mercury in leaves of common deciduous tree species in Minnesota, USA. Environ Sci Technol 47(18):10462–10470

Larssen T, de Wit HA, Wiker M, Halse K (2008) Mercury budget of a small forested boreal catchment in southeast Norway. Sci Total Environ 404(2–3):290–296

Manceau A, Wang J, Rovezzi M, Glatzel P, Feng X (2018) Biogenesis of mercury–sulfur nanoparticles in plant leaves from atmospheric gaseous mercury. Environ Sci Technol 52(7):3935–3948

Mazur M, Mitchell CPJ, Eckley CS, Eggert SL, Kolka RK, Sebestyen SD, Swain EB (2014) Gaseous mercury fluxes from forest soils in response to forest harvesting intensity: a field manipulation experiment. Sci Total Environ 496:678–687

Melendez-Perez JJ, Fostier AH, Carvalho JA Jr, Windmöller CC, Santos JC, Carpi A (2014) Soil and biomass mercury emissions during a prescribed fire in the Amazonian rain forest. Atmos Environ 96:415–422

Millhollen AG, Gustin MS, Obrist D (2006) Foliar mercury accumulation and exchange for three tree species. Environ Sci Technol 40(19):6001–6006

Moore C, Carpi A (2005) Mechanisms of the emission of mercury from soil: role of UV radiation. J Geophys Res. https://doi.org/10.1029/2004JD005567

Nasr M, Arp PA (2015) Biomonitoring and assessing total mercury concentrations and pools in forested areas. Biomonitoring 2(1):47–63

Nottingham AT, Whitaker J, Turner BL, Salinas N, Zimmermann M, Malhi Y, Meir P (2015) Climate warming and soil carbon in tropical forests: insights from an elevation gradient in the Peruvian Andes. Bioscience 65(9):906–921

Obrist D, Kirk JL, Zhang L, Sunderland EM, Jiskra M, Selin NE (2018) A review of global environmental mercury processes in response to human and natural perturbations: changes of emissions, climate, and land use. Ambio 47(2):116–140

Osterwalder S, Bishop K, Alewell C, Fritsche J, Laudon H, Åkerblom S, Nilsson MB (2017) Mercury evasion from a boreal peatland shortens the timeline for recovery from legacy pollution. Sci Rep 7(1):16022

Park SY, Kim PR, Han YJ (2013) Mercury exchange flux from two different soil types and affecting parameters. Asian J Atmos Environ 7(4):199–208

Rea AW, Lindberg SE, Scherbatskoy T, Keeler GJ (2002) Mercury accumulation in foliage over time in two northern mixed-hardwood forests. Water Air Soil Pollut 133(1–4):49–67

Risch MR, DeWild JF, Gay DA, Zhang L, Boyer EW, Krabbenhoft DP (2017) Atmospheric mercury deposition to forests in the eastern USA. Environ Pollut 228:8–18

Różański SŁ, Castejón JMP, Fernández GG (2016) Bioavailability and mobility of mercury in selected soil profiles. Environ Earth Sci 75(13):1065

Rustad LE, Campbell JL (2012) A novel ice storm manipulation experiment in a northern hardwood forest. Can J For Res 42(10):1810–1818

Rutter AP, Schauer JJ, Shafer MM, Creswell JE, Olson MR, Robinson M, Collins RM, Parman AM, Katzman TL, Mallek JL (2011) Dry deposition of gaseous elemental mercury to plants and soils using mercury stable isotopes in a controlled environment. Atmos Environ 45(4):848–855

Sanders-DeMott R, Sorensen PO, Reinmann AB, Templer PH (2018) Growing season warming and winter freeze–thaw cycles reduce root nitrogen uptake capacity and increase soil solution nitrogen in a northern forest ecosystem. Biogeochemistry 137(3):337–349

Schroeder WH, Munthe J, Lindqvist O (1989) Cycling of mercury between water, air, and soil compartments of the environment. Water Air Soil Pollut 48(3–4):337–347

Schroeder WH, Beauchamp S, Edwards G, Poissant L, Rasmussen P, Tordon R, Dias G, Kemp J, Van Heyst B, Banic CM (2005) Gaseous mercury emissions from natural sources in Canadian landscapes. J Geophys Res. https://doi.org/10.1029/2004JD005699

Schwesig D, Ilgen G, Matzner E (1999) Mercury and methylmercury in upland and wetland acid forest soils of a watershed in NE-Bavaria, Germany. Water Air Soil Pollut 113(1–4):141–154

Selin NE, Jacob DJ, Park RJ, Yantosca RM, Strode S, Jaeglé L, Jaffe D (2007) Chemical cycling and deposition of atmospheric mercury: global constraints from observations. J Geophys Res. https://doi.org/10.1029/2006JD007450

Sheehan KD, Fernandez IJ, Kahl JS, Amirbahman A (2006) Litterfall mercury in two forested watersheds at Acadia National Park, Maine, USA. Water Air Soil Pollut 170(1–4):249–265

Sheffield J, Wood EF (2008) Projected changes in drought occurrence under future global warming from multi-model, multi-scenario, IPCC AR4 simulations. Clim Dyn 31(1):79–105

Sigler JM, Lee X (2006) Gaseous mercury in background forest soil in the northeastern United States. J Geophys Res. https://doi.org/10.1029/2005JG000106

Skyllberg U, Xia K, Bloom PR, Nater EA, Bleam WF (2000) Binding of mercury (II) to reduced sulfur in soil organic matter along upland-peat soil transects. J Environ Qual 29(3):855–865

Smith-Downey NV, Sunderland EM, Jacob DJ (2010) Anthropogenic impacts on global storage and emissions of mercury from terrestrial soils: insights from a new global

model. J Geophys Res. https://doi.org/10.1029/2009JG001124

St. Louis VL, Rudd JW, Kelly CA, Hall BD, Rolfhus KR, Scott KJ, Lindberg SE, Dong W (2001) Importance of the forest canopy to fluxes of methyl mercury and total mercury to boreal ecosystems. Environ Sci Technol 35(15):3089–3098

Stoken OM, Riscassi AL, Scanlon TM (2016) Association of dissolved mercury with dissolved organic carbon in US rivers and streams: the role of watershed soil organic carbon. Water Resour Res 52(4):3040–3051

Templer PH, Reinmann AB, Sanders-DeMott R, Sorensen PO, Bowles F, Sofen LE, Harrison JL, Halm I, Rustad L, Martin ME, Grant N (2017) Climate change across seasons experiment (CCASE): a new method for simulating future climate in seasonally snow-covered ecosystems. PLoS ONE 12(2):e0171928

US Environmental Protection Agency (1996) Method 1669: sampling ambient water for trace metals at EPA water quality criteria levels. Environmental Protection Agency, Washington, DC

US Environmental Protection Agency (1998) Mercury in solids and solutions by thermal decomposition, amalgamation, and atomic absorption spectropho-tometry. Environmental Protection Agency, Washington, DC

US Environmental Protection Agency (2002) Method 1631, Revision E: Mercury in water by oxidation, purge and trap, and cold vapor atomic fluorescence spectrometry. US Environmental Protection Agency, Washington, DC

Vadeboncoeur MA, Hamburg SP, Yanai RD, Blum JD (2014) Rates of sustainable forest harvest depend on rotation length and weathering of soil minerals. For Ecol Manag 318:194–205

Wang X (2012) Seasonal variations in the inputs and fate of mercury in a Northern hardwood forest. Master Thesis at Syracuse University

Wieser G, Grams TE, Matyssek R, Oberhuber W, Gruber A (2015) Soil warming increased whole-tree water use of Pinus cembra at the treeline in the Central Tyrolean Alps. Tree Physiol 35(3):279–288

Wright LP, Zhang L, Marsik FJ (2016) Overview of mercury dry deposition, litterfall, and throughfall studies. Atmos Chem Phys 16(21):13399–13416

Xu JX, Xue L, Su ZY (2016) Impacts of forest gaps on soil properties after a severe ice storm in a *Cunninghamia lanceolata* stand. Pedosphere 26(3):408–416

Yang YK, Zhang C, Shi XJ, Tao LIN, Wang DY (2007) Effect of organic matter and pH on mercury release from soils. J Environ Sci 19(11):1349–1354

Yang Y, Yanai RD, Montesdeoca M, Driscoll CT (2017) Measuring mercury in wood: challenging but important. Int J Environ Anal Chem 97(5):456–467

Yang Y, Yanai RD, Driscoll CT, Montesdeoca M, Smith KT (2018) Concentrations and content of mercury in bark, wood, and leaves in hardwoods and conifers in four forested sites in the northeastern USA. PLoS ONE 13(4):e0196293

Yu X, Driscoll CT, Warby RA, Montesdeoca M, Johnson CE (2014) Soil mercury and its response to atmospheric mercury deposition across the northeastern United States. Ecol Appl 24(4):812–822

Zhang HA, Lindberg SE (1999) Processes influencing the emission of mercury from soils: a conceptual model. J Geophys Res 104(D17):21889–21896

Zhang H, Lindberg SE, Marsik FJ, Keeler GJ (2001) Mercury air/surface exchange kinetics of background soils of the Tahquamenon River watershed in the Michigan Upper Peninsula. Water Air Soil Pollut 126(1–2):151–169